Atp1a2 and Kcnj9 are candidate genes underlying oxycodone behavioral sensitivity and withdrawal in C57BL/6 substrains

Lisa R. Goldberg[1,2], Britahny M. Baskin[1,3], Yahia Adla[1], Jacob A. Beierle [1,2,4], Julia C. Kelliher[1], Emily J. Yao[1], Stacey L. Kirkpatrick[1], Eric R. Reed[5], David F. Jenkins[5], Alexander M. Luong[1], Kimberly P. Luttik[1], Julia A. Scotellaro[1,6], Timothy A. Drescher[1], Sydney B. Crotts[1], Neema Yazdani[1,2,4], Martin T. Ferris[7], W. Evan Johnson[8], Megan K. Mulligan[9], Camron D. Bryant[1,3*]

[1]Laboratory of Addiction Genetics, Department of Pharmaceutical Sciences and Center for Drug Discovery, Northeastern University, Boston, MA USA
[2]Graduate Program in Biomolecular Pharmacology, Department of Pharmacology, Physiology & Biophysics, Boston University Chobanian and Avedisian School of Medicine, Boston, MA USA
[3]T32 Training Program on Development of Medications for Substance Use Disorder, Center for Drug Discovery, Northeastern University
[4]Transformative Training Program in Addiction Science, Boston University
[5]Graduate Program in Bioinformatics, Boston University, Boston, MA USA
[6] Undergraduate Research Opportunity Program (UROP), Boston University
[7]Department of Genetics, University of North Carolina, Chapel Hill, NC USA
[8]Division of Infectious Disease, Department of Medicine, Center for Data Science, Rutgers University, New Jersey, USA
[9]Department of Genetics, Genomics, and Informatics, University of Tennessee Health Science Center, Memphis, TN USA

Running title:
Atp1a2 and Kcnj9 are candidate genes for opioid behaviors

*Corresponding Author
Camron D. Bryant, Ph.D.
Laboratory of Addiction Genetics
Department of Pharmaceutical Sciences
Center for Drug Discovery
Northeastern University
140 The Fenway
X138
Boston, MA USA 02115
E: c.bryant@northeastern.edu
P: (617)-373-7663

ABSTRACT

Opioid use disorder is heritable, yet its genetic etiology is largely unknown. Analysis of addiction model traits in rodents (e.g., opioid behavioral sensitivity and withdrawal) can facilitate genetic and mechanistic discovery. C57BL/6J and C57BL/6NJ substrains have extremely limited genetic diversity, yet can show reliable phenotypic diversity which together, can facilitate gene discovery. The C57BL/6NJ substrain was less sensitive to oxycodone (OXY)-induced locomotor activity compared to the C57BL/6J substrain. Quantitative trait locus (QTL) mapping in an F2 cross identified a distal chromosome 1 QTL explaining 7-12% of the variance in OXY locomotor sensitivity and anxiety-like withdrawal in the elevated plus maze. We identified a second QTL for withdrawal on chromosome 5 near the candidate gene Gabra2 (alpha-2 subunit of GABA-A receptor) explaining 9% of the variance. Next, we generated recombinant lines from an F2 founder spanning the distal chromosome 1 locus (163-181 Mb), captured the QTL for OXY sensitivity and withdrawal, and fine-mapped a 2.45-Mb region (170.16-172.61 Mb). There were five striatal cis-eQTL transcripts in this region (Pcp4l1, Ncstn, Atp1a2, Kcnj9, Igsf9), two of which were confirmed at the protein level (KCNJ9, ATP1A2). Kcnj9, a.k.a., GIRK3, codes for a potassium channel that is a major effector of mu opioid receptor signaling. Atp1a2 codes for a subunit of a Na+/K+ ATPase enzyme that regulates neuronal excitability and shows adaptations following chronic opioid administration. To summarize, we identified genetic sources of opioid behavioral differences in C57BL/6 substrains, two of the most widely and often interchangeably used substrains in opioid addiction research.

INTRODUCTION

Opioid use disorder (OUD) is an epidemic in the United States that was fueled by the overprescribing and misuse of the highly addictive mu opioid receptor agonist oxycodone (**OXY**; active ingredient in Oxycontin®)[1]. The switch to the abuse-deterrent formulation led to a shift toward illicit use of heroin[2] and then the more potent compound fentanyl[3]. Opioid-related deaths have surpassed 100,000 per year (U.S. CDC, 2023; https://www.cdc.gov/opioids/basics/epidemic.html). Twin studies estimate that the heritability of opioid dependence is around 50%[4,5], however the genetic basis remains largely unknown[6–8]. Both shared and distinct genetic factors and biological mechanisms are likely to contribute to the progressive stages of opioid addiction, including initial sensitivity to the neurobehavioral properties (e.g., interoception, reward, reinforcement), tolerance, withdrawal (physical, motivational, emotional-affective) and alleviation of withdrawal or craving with agonist treatment. Human genetic studies support distinct genetic factors underlie variation in the frequency and amount of drug use and symptoms that define drug dependence[6].

Genetic factors influencing initial sensitivity to the subjective and behavioral responses to addictive drugs can often predict behaviors associated with progressive stages of addiction. One measure of drug sensitivity is locomotor stimulation induced by addictive drugs, a behavior mediated by shared neural circuitry and neurochemistry with reward and reinforcement, including dopamine release in the dorsal and ventral striatum[9–11]. In genetic support of these observations, we mapped quantitative trait loci (QTLs) and candidate genes underlying acute sensitivity to psychostimulants and opioids (e.g., *Csnk1e*, *Hnrnph1*) and confirmed their involvement in conditioned reward (e.g., conditioned place preference; **CPP**) and operant reinforcement (e.g., self-administration)[12–16]. Gene knockout studies support a shared influence of acute drug response with reward, reinforcement, and progressive behavioral models for addiction[17]. In sum, genetic mapping of acute behavioral sensitivity to addictive drugs is a high throughput approach to finding genes with a predictable influence on drug reward, reinforcement, and likely other addiction model traits (e.g., withdrawal).

In considering genetic crosses for rapid gene mapping and discovery, C57BL/6J (**B6J**) and C57BL/6NJ (**B6NJ**) are two of the most commonly used substrains in biomedical research. B6J and B6NJ are nearly 100% genetically identical, yet exhibit significant differences in several addiction model traits[18], including ethanol consumption[19–21], psychostimulant-induced locomotor activity and sensitization[22,23], nicotine-induced locomotor activity, hypothermia, antinociception, and anxiety-like behavior[24], conditioned place aversion induced by the mu opioid receptor antagonist naloxone[25], and binge-like eating[26,27]. While phenotypic differences between B6 substrains can be quite large [18,28,29], genotypic diversity is extremely small[29–33]. Together, reliable, robust phenotypic variance and extremely reduced genetic complexity are ideal for behavioral QTL and expression QTL (eQTL) analysis in an F2 reduced complexity cross (**RCC**) analysis and can facilitate candidate gene nomination and causal variant identification[34,35].

Multiple examples in RCCs show their power in gene discovery for complex traits. Kumar and colleagues used an RCC between C57BL/6 substrains to map a QTL for cocaine locomotor sensitization to a missense mutation in *Cyfip2*[22]. We also mapped the same locus for methamphetamine-induced locomotor

activity (maximum speed)[23] and ten again mapped and validated the same locus/gene for another trait - binge-like eating of sweetened palatable food[26]. In another example involving RCCs, Mulligan and colleagues used the BXD recombinant inbred lines combined with analysis of closely related C57BL/6 substrains to identify a functional intronic variant in Gabra2 (alpha-2 subunit of the GABA-A receptor) that reduced mRNA and protein expression[36]. Genetic mapping by our group, followed by validation using genetically engineered lines, demonstrated that the Gabra2 variant was responsible for substrain differences in acute methamphetamine-induced locomotor activity that was more pronounced in male mice[37]. Finally, Phillips and colleagues exploited the reduced genetic complexity between DBA/2J substrains to identify a functional missense mutation in *Taar1* that influences methamphetamine-induced hyperthermia, negative reinforcement, and toxicity[38–42]. Our lab also extended the RCC approach to BALB/c substrains, where we quickly identified candidate genes for nociceptive sensitivity, brain weight, and opioid behavioral and molecular traits[43,44].

In the present study, we examined oxycodone behavioral sensitivity and withdrawal in a B6J x B6NJ-F2 RCC. Upon identifying a major distal chromosome 1 QTL for oxycodone behavioral sensitivity and withdrawal, we implemented an efficient strategy to generate recombinant lines within the QTL interval[34], and refined it to a 2.45-Mb region. We then sourced a historical striatal expression QTL dataset from the same genetic cross[23,45] to home in on functionally plausible candidate genes. Finally, we conducted immunoblot analysis of eQTL genes within a recombinant line capturing the behavioral QTL, providing further support for candidate causal genes. The results provide multiple positional loci and highly plausible candidate genes underlying opioid behavioral sensitivity and withdrawal.

MATERIALS AND METHODS

Materials and Methods are all provided in the Supplementary Material.

RESULTS

Reduced OXY locomotor sensitivity in B6NJ versus B6J substrains

A schematic of the OXY-CPP protocol is shown in **Fig.1A**. Because there was a small amount of missing data across days, sample sizes per figure panel are provided in **Fig.S1**. Day(D)2 was the first OXY training day following assessment of initial preference on D1 (SAL). In examining OXY-induced locomotor activity on D2, there was a Dose effect ($F_{3,293}=176.2$; $p<0.0001$), but no Substrain effect ($F_{1,293}=1.66$; $p=0.20$) and no interaction ($F_{3,293}<1$). Bonferroni post-hoc indicated the effect of Dose was explained by an increase in distance (m) at 1.25mg/kg versus 0mg/kg (**p<0.01) and the 5mg/kg dose versus 0mg/kg (****p<0.0001; **Fig.1B**). The Dose effect was also explained by an increase in distance following 5mg/kg versus both 0.6125mg/kg (****p<0.0001) and 1.25mg/kg (****p<0.0001; **Fig.1B**).

In examining the time course of OXY locomotion (1.25 mg/kg, i.p.) in 5-min bins, there was a Substrain effect ($F_{1,150}=8.07$; **p<0.01), indicating reduced OXY distance in B6NJ versus B6J (**Fig.1C**). There was also a Time effect ($F_{5,150}=39.63$; ****p<0.0001), but no interaction ($F_{5,150}<1$).

For the second OXY training dose on D4, there was a Dose effect (F3,291=386.2; ****p<0.0001) but no Substrain effect (F1,291<1) and no interaction (F3,291=1.11; p=0.35). The Dose effect was explained by increased OXY distance at 1.25mg/kg versus 0mg/kg (***p<0.001), at 5mg/kg versus 0mg/kg (****p<0.0001), at 1.25 mg/kg versus 0.6125 mg/kg (*p < 0.05), and at 5 mg/kg versus 1.25 mg/kg (****p<0.0001; **Fig.1D**).

In examining the time course of OXY locomotion (1.25 mg/kg, i.p.) on D4 in 5-min bins, there was a Subsrain effect (F1,150=8.46; **p<0.01; B6NJ<B6J; **Fig.1E**), indicating and overall decrease in OXY-induced locomotor activity in B6NJ versus B6J. There was also a Time effect (F5,150=52.30; ****p<0.0001) but no interaction (F5,150=1.65; p=0.15).

Importantly, we also examined Substrain and Dose effects on SAL training days for OXY-CPP (D3,D5) and found little evidence for Substrain effects (**Fig.S2**). These results support decreased OXY locomotion on D2 and D4 in B6NJ versus B6J mice, providing the impetus for genetic analysis in an RCC. In further support, narrow-sense h2 estimates[46] based on between-strain (genetic), within-strain (environmental), and total variance were 0.22 and 0.31 for D2 and D4 OXY locomotion, respectively.

Drug-free (D8-D1) and state-dependent OXY-CPP (D9-D1) in B6 substrains

Following initial preference assessment (D1) and training days (D2 through D5), we assessed drug-free OXY-CPP following saline injections on D8 and state-dependent OXY-CPP following subsequent training doses on D9 via change in time spent on the OXY-paired side (s) compared to D1. In examining drug-free OXY-CPP on D8, there was a Dose effect (F3,293=5.52; **p< 0.01) but no Substrain effect (F3,293<1) and no interaction (F3,293<1). The Dose effect was explained by increased OXY-CPP from 0mg/kg to 0.6125mg/kg (*p<0.05) and from 0 mg/kg to 5mg/kg (**p<0.01; **Fig.1F**). While these results demonstrate significant drug-free OXY-CPP, they do not support a Substrain effect.

In examining state-dependent OXY-CPP on D9, there was a significant Dose effect (F3,269=17.56; *p<0.0001). However, there was no Substrain effect (F1,269<1) and no interaction (F3,269<1). The Dose effect was explained by increased OXY-CPP at 1.25mg/kg (***p<0.001) and 5mg/kg versus 0 mg/kg (****p<0.0001) and at 5mg/kg versus 0.6125mg/kg (**p<0.01; **Fig.1G**). Thus, state-dependent CPP did not depend on Substrain.

QTL mapping of OXY locomotion and withdrawal

A list of the polymorphic markers for QTL mapping is provided in **Table S1**. We identified a single QTL on distal chromosome 1 for OXY locomotion on D2 (**Fig.2A-D**). The effect plot mirrored the parental substrain difference, where mice containing one or two copies of the B6NJ allele (J/N, N/N) at the peak-associated marker showed a decrease in OXY locomotion (**Fig.2D**). The same QTL was also significant for D2 spins (mouse nose/body spinning 360 degrees around in a circle) and D2 rotations (circling all four quadrants) as well as D4 Spins and D4 Rotations (**Fig.2A-C**) and the allelic effects on phenotypes were all in the same direction as D2 distance (N<J; **Fig.S3A-F**). Important, the Genotype effect on locomotor activity at this QTL

was restricted to the OXY group (**Fig.2C**). These effect plots all support a dominant model of inheritance, with inheritance of one copy of the N allele (J/N) being sufficient to decrease OXY-induced locomotor activity to its minimal level (**Fig.2D**). The same locus was also significant for two out of the three same phenotypes on D4, namely D4 Spins and D4 Rotations (**Fig.2A-C**). These results provide strong support for a causal gene/variant within this locus underlying OXY locomotion.

A subset of F_2 mice above subsequently underwent eight additional injections of high-dose OXY (20 mg/kg, i.p.) or SAL (i.p.) over 2 weeks (see OXY regimen in Supplementary Material). Sixteen hours after the final injection, F2 mice were tested during spontaneous OXY withdrawal on the EPM, a behavioral assay modeling anxiety-like behavior[47]. We identified a QTL on distal chromosome 1 (Open Arm Entries, Open Arm Distance, % Open Arm Time; **Fig.2E-G**) that was similarly localized as the QTL for OXY-induced locomotor activity (**Table 1, Fig.1A,B**) and suggests a common causal gene/variant. In support, the effect plot indicated that OXY-trained mice with the J/J allele (greater OXY sensitivity) at the peak chromosome 1-associated marker (rs51237371, 181.32 Mb) showed an OXY-dependent increase in Open Arm Entries compared to SAL-trained mice with the J/J allele, while there was no effect of OXY in mice with the N/N allele (**Fig.2G**). A similar distal chromosome 1 effect plot for Open Arm Distance was observed (**Fig.S3G**). Despite the J/J-dependent OXY-induced increase in open arm behaviors, all OXY-trained mice spent less % time in the open arms compared to SAL-trained mice, as indicated by the distal chromosome 1 effect plot (**Fig.S3H**).

We identified a second QTL that was localized to medial chromosome 5 (Open Arm Entries; **Fig.2E,H,I**). OXY-trained J/J mice at the peak chromosome 5-linked marker (rs33209545, 59.83 Mb) again showed an increase in Open Arm Entries, while the N/N genotype was not responsive to OXY (**Fig.2I**). This QTL is proximal to *Gabra2* (codes for alpha-2 subunit of GABA-A receptor), a well-known cis-eQTL mediated by a single intronic deletion near a splice acceptor site that is private to the B6J substrain[36]. This mutation is genetically linked to several neurobehavioral traits, including methamphetamine stimulant sensitivity[23] and modification of seizures in Dravet syndrome Scn8 encephalopathy models[48,49]. *Gabra2* is a high-priority candidate gene for spontaneous opioid withdrawal, given that the alpha-2 subunit is a major molecular component of the anxiogenic and anxiolytic properties benzodiazepine-site drugs, alcohol dependence, and polydrug misuse[50].

Distal chromosome 1 recombinant lines spanning 163 Mb to 181 Mb resulting from repeated backcrossing to B6J

Because the distal chromosome 1 QTL spanned a large region (**Fig.2A**), we sought to rapidly narrow this locus by generating and phenotyping interval-specific recombinant lines spanning 163-181 Mb at each generation of backcrossing[34]. Details on the resultant recombinant lines that were generated through repeated backcrossing, monitoring, and phenotyping of the163-181 Mb region are provided in **Supplementary Material**. Briefly, eight recombinant lines were generated, including the N6-1 line spanning 163-181 Mb as well as various lines arising from either N6-1 or independently as separate lineages to span the entire interval. **See**

Tables S2 and S3 and Figure S4 for information on markers, recombination break points, pedigree, and sample sizes.

Capture of the distal chromosome 1 QTL influencing OXY behavioral sensitivity and withdrawal in the N6-1 recombinant line

A schematic is shown for the N6-1 recombinant region on distal chromosome 1 in **Fig.3A**. The heterozygous region conservatively spanned 163.13-181.32 Mb, meaning that N6-1 mice were homozygous for B6J at the most proximal and distal markers. The sample sizes are provided in **Fig.S5**. In examining locomotor activity during initial preference assessment following SAL (i.p.) on D1 (prior to OXY training), N6-1 heterozygotes (J/N) showed a small reduction in D1 locomotor activity versus B6J wild-type littermates (J/J) ($t_{132}=2.12$; *p=0.036; **Fig.3B**).

In examining OXY-induced locomotor activity on D2, there was an effect of Genotype ($F_{1,31}=11.36$; **p<0.01), Treatment ($F_{1,131}=63.66$;****p<0.0001), and an interaction ($F_{1,131}=4.56$;*p<0.05). Bonferroni post-hoc indicated a significant decrease in OXY-induced locomotor activity in J/N versus J/J (***p<0.001), Both OXY genotypes showed an increase in locomotor activity versus their SAL counterparts (****p<0.0001,***p<0.001, respectively; **Fig.3C**). Thus, we successfully captured the distal chromosome 1 QTL for OXY behavioral sensitivity on D2. Similarly to the parental substrains, we examined the time course of the D2 OXY response in 5-min bins across 30 min. There was a main effect of Genotype ($F_{1,114}=9.58$; **p<0.01), Treatment ($F_{1,114}=55.43$; ****p<0.0001), Time ($F_{5,570}=118.00$; p<0.0001), a Genotype x Time interaction ($F_{1,114}=3.66$; **p<0.01), and a Treatment x Time interaction ($F_{5,570}=25.67$; p<0.0001). However, neither the Genotype x Treatment nor the Genotype x Treatment x Time were significant (ps=0.17,0.29; **Fig.3D**).

In examining OXY-induced locomotor activity on D4, there was a Treatment effect ($F_{1,131}=80.00$; ****p<0.0001) but no Genotype effect ($F_{1,131}<1$) and no interaction ($F_{1,131}<1$; **Fig.3E**). In examining the examining the time course of the D4 OXY response in 5-min bins across 30 min, there was no Genotype effect, nor was there any two- or three-way interaction of Genotype with Treatment and/or Time (ps>0.05). However, there was a Treatment effect ($F_{1,130}=77.60$;****p<0.0001), a Time effect ($F_{5,650}=128.80$; *p<0.0001), and an interaction ($F_{5,650}=47.88$; p<0.0001, indicating time-dependent OXY-induced locomotion (**Fig.3F**).

In examining drug-free OXY-CPP on D8 (D8-D1,s), there was a Treatment effect ($F_{1,130}=6.91$;**p<0.01) but no Genotype effect ($F_{1,130}=1.76$;p=0.19) and no interaction ($F_{1,130}<1$). In examining state-dependent OXY-CPP on D9 (D9-D1,s), there was a Treatment effect ($F_{1,131}=5.23$; *p<0.05) but no Genotype effect ($F_{1,131}=2.84$; p=0.095) and no interaction ($F_{1,131}<1$), together indicating that OXY induced significant drug-free and state-dependent CPP versus SAL treatment, irrespective of Genotype (**Fig.3G,H**).

In examining EPM behaviors during spontaneous OXY withdrawal, we considered three behaviors with a distal chromosome 1 QTL (% Open Arm Time, Open Arm Entries, and Open Arm Distance; **Fig.2E,F**). For %

Open Arm Time, there was no effect of Genotype ($F_{1,70}<1$), Treatment ($F_{1,70}<1$), or interaction ($F_{1,70}<1$; **Fig.3I**). For Open Arm Entries, while there was no Genotype effect ($F_{1,70}=1.10$; $p=0.30$), there was a Treatment effect ($F_{1,70}=4.90$; $^{*}p<0.05$) and most importantly, there was a Genotype x Treatment interaction ($F_{1,70}=5.79$; $p<0.05$). Bonferroni post-hoc indicated a significant decrease in Open Arm Entries in OXY J/J mice vs SAL J/J ($^{*}p<0.05$), with no significant difference between J/N OXY mice vs. J/N SAL mice ($p>0.05$). Interestingly, while this result indicated that the OXY-responsive allele was once again linked to J/J, the direction of Genotype effect was opposite versus F2 mice, resulting in a decrease in open arm entries (**Fig.3J**) rather than an increase (**Fig.2G**). For Open Arm Distance, there was no effect of Genotype ($F_{1,70}<1$), Treatment ($F_{1,70}<1$), or interaction ($F_{1,70}<1$; **Fig.3K**).

Fine mapping the distal chromosome 1 behavioral QTL for D2 OXY behavioral sensitivity in recombinant lines

Given the sheer number of recombinant lines (**Table S3; Fig.S4**), it was clear that an abbreviated, two-day protocol would be more efficient to test for capture of the OXY behavioral QTLs observed on D2 (following 1.25 mg/kg OXY on the OXY-paired side; **Fig.2A-D**). Therefore, phenotyping of recombinant lines below was limited to D1 and D2 of the OXY-CPP protocol. Sample sizes are provided in **Fig.S4B**. A Bonferroni-corrected p-value was employed to adjust for comparisons across eight recombinant lines ($p<0.05/8=0.00625$). Significant results are reported below. Non-significant results are included in **Supplementary Material**.

In examining D1 Distance following SAL (i.p.), only **N6-1** showed a Genotype effect, with J/N showing a decrease ($t_{48}=3.35$; $^{**}p=0.0016$; **Fig.4B**). In examining D1 Rotations following SAL (i.p.), again, only **N6-1** showed a Genotype effect, with a decrease in J/N ($t_{48}=2.87$; $^{**}p=0.0061$; **Fig.4C**; vertically below panel B). In examining D1 Spins following SAL (i.p.), none of the recombinant lines showed a Genotype effect (ps > 0.038).

In examining D2 OXY locomotion, two recombinant lines showed a significant decrease with J/N, including **N6-1** ($t_{48}=4.29$;$^{****}p<0.0001$) and **N9-8** ($t_{49}=4.09$;$^{***}p=0.0002$; **Fig.4E**). In examining D2 OXY rotations, again, the same two lines showed a decrease with J/N, including **N6-1** ($t_{48}=4.36$;$^{****}p<0.0001$) and **N9-8** ($t_{49}=3.54$;$^{***}p=0.0009$; **Fig.4F**; vertically below panel E). In examining D2 OXY spins, the same two lines showed significant decrease with J/N, including **N6-1** ($t_{48}=3.65$;$^{***}p=0.0006$) and **N9-8** ($t_{49}=3.60$;$^{***}p=0.0007$; **Fig.4G**; vertically below panel F).

In considering the recombination breakpoints of the two recombinant lines that captured the D2 OXY traits ("+": N6-1, N9-8) versus the six congenic lines that failed to capture the QTL ("-": N5-10, N5-11, N5-8, N7-15, N8-7, and N9-5), the proximal breakpoint of N9-8 which captured the QTL ("+") ended conservatively at the most proximal marker genotyped as J/N, namely rs255914894 (172.61 Mb; **Fig.4A**). The distal breakpoint of N7-15 line which failed to capture the QTL ("-") ended conservatively at the most distal marker genotyped at J/N, namely rs3705254 (170.16 Mb; **Fig.4A**). These two key observations, combined with the other more distal recombinant lines that failed to capture the QTL (e.g., N5-10,-11,-8) reduced the causal locus to a 2.45-Mb region spanning 170.16-172.61 Mb (**Fig.4A**). Note that although the N8-7 and N9-5 lines that failed to capture

the QTL, both appear to possess the same proximal breakpoint as N9-8 which captured the QTL (**Fig.4A**), these two lines emerged as two independent recombinations from N6-1 (**Fig.S4A; Table S3**) and thus have two different proximal breakpoints. These two break points are also distinct from the proximal recombination from N9-8 which captures the QTL. Both N8-7 and N9-5 showed a trend toward partially capturing the QTL for decreased OXY-induced behaviors. Given tha large sample sizes were employed for each of the three lines (**Fig.S4B**) and thus statistical power is unlikely a limitation (see Power Analysis in **Supplementary Material**), one explanation is that there are multiple variants within the locus and that the N9-8 line fully captures whereas the N8-7 N9-5 lines only partially capture, due to shorter proximal extensions of the recombinant segments. Unfortunately, despite our extensive efforts in surveying over 100 additional potential markers, we were unable to validate any polymorphic variants within the positionally cloned 170.16-172.61 Mb interval due to a variety of reasons, including repeated failure in PCR amplification and Sanger sequencing, and previously reported polymorphic SNPs that were false-positives and we genotyped as monomorphic. The widespread failure in Sanger sequencing could be due to uncharacterized structural variation segregating within this region. A UCSC genome browser snapshot of the genes within the 2.45 Mb interval is provided in **Fig.S6**.

Cis-expression QTLs

Genetic regulation of gene expression (eQTLs) provides a functional link and causal support for quantitative trait genes/variants underlying behavior[23,43,44,51]. Using a striatal RNA-seq dataset from 23 F2 mice that had undergone OXY-CPP testing, two weeks of high-dose OXY treatment (20 mg/kg, i.p. 8X), and spontaneous OXY withdrawal 16 h after the final 20 mg/kg OXY injection[23,45], we focused on cis-eQTL transcripts on chromosome 1 showing a peak association with OXY behavior (rs51237371; 181.32 Mb). There were five transcripts within the positionally cloned 170.16-172.61 Mb region that met this criterion: Pcp4l1, Ncstn, Atp1a2, Kcnj9, and Igsf9 (**Fig.5A**). There were also three cis-eQTLs distal to the 2.45-Mb region that could potentially be regulated by one or more noncoding variants within the 2.45-Mb region and thus, are potential (although less likely) candidate genes, including Cadm3, Aim2, and Rgs7 (**Fig.5A**). A larger list of 58 transcripts possessing a peak cis-eQTL with rs51237371 is provided in **Table S4**.

We next focused on cis-eQTLs within the chromosome 5 QTL for Open Arm Entries during OXY withdrawal (**Fig.2A,E,H,I**). A list of transcripts showing cis-eQTLs that peak with the behavioral QTL marker (rs32809545; chromosome 5: 59.83 Mb) is provided in **Table S5**. There were five sequential eQTL transcripts within less than 20 Mb of the peak marker, including Cpeb2, N4bp2, Gabra4, Pdgfra, and Clock. Perhaps most noteworthy is that the chromosome 5 behavioral QTL (peak=59.83 Mb) is just adjacent to the peak cis-eQTL (rs29547790; 70.93 Mb) for expression of Gabra2 (alpha-2 subunit of the GABA-A receptor), a GABA-A receptor subunit with a well-established role in anxiety and the anxiolytic effects of benzodiazepines[50,52]. We identified the causal mutation for loss of Gabra2 expression in the B6J substrain, which comprises a single nucleotide deletion near a splice acceptor site[36] and have mapped and validated this mutation for other traits, including methamphetamine stimulant sensitivity[23] and modification of seizure phenotypes in experimental

models[48,49]. Given the increasing examples implicating this Gabra2 eQTL, we also considered cis-eQTLs that peak at rs29547790 (70.93 Mb) as potential candidate genes. The list of transcripts showing peak eQTLs with rs29547790 is published[23]. The top eQTL linked to rs29547790 is Gabra2.

Striatal immunoblot analysis in the N6-1 recombinant line supports Atp1a2 and Kcnj9 as candidate genes underlying OXY locomotion and withdrawal

There were five transcripts with cis-eQTLs within the 2.45 Mb interval (Pcp4l1, Ncstn, Atp1a2, Kncj9, and Igsf9) and an additional three cis-eQTL-containing transcripts just distal to the 2.45-Mb region (Cam3, Aim2, Rgs7; **Fig.5A**). We ran striatal immunoblot analysis from naive N6-1 mice on proteins encoded by four out of the five transcripts with cis-eQTLs in the 2.45 Mb locus (PCP4L1, ATP1A2, KCNJ9, and IGSF9; **Fig.5B-E**). We could not obtain reliable blots for fifth protein, nicastrin (NCSTN). There was a significant increase in ATP1A2 immunostaining in J/N (t22=4.59; ***p=0.00014; **Fig.5C**) and a significant decrease in KCNJ9 immumostaining in J/N (t18=2.21; *p=0.04; **Fig.5D**). There was no significant difference with PCP4L1 (t22=1.02;p=0.32) or IGSF9 (t22<1; **Fig.5E**). We assayed 3 additional proteins encoded by transcripts with cis-eQTLs that were distal to the fine-mapped 2.45 Mb locus (CADM3, AIM2, RGS7; **Fig.5F-H**). There was a significant increase in AIM2 in J/N (t22=3.57; **p=0.0017; **Fig.5G**) and a trending, non-significant increase in the expression of RGS7 in J/N (t19=1.80; p=0.088; **Fig.5H**). There was no significant genotypic difference in immunostaining of CADM3 (t22=1.45; p=0.16; **Fig.5F**). To summarize, we identified two compelling candidate genes within the fine-mapped locus (ATP1A2, KCNJ9) that show genotype-dependent changes in expression at both the transcript and protein levels.

DISCUSSION

We employed a C57BL/6 RCC combined with fine-mapping, cis-eQTL mapping, and protein analysis to triangulate on two compelling candidate genes underlying OXY locomotion and withdrawal – Atp1a2 and Kcnj9. We also identified a second locus and candidate gene on chromosome 5 for opioid withdrawal, namely Gabra2. For the distal chromosome 1 locus, we implemented a novel fine-mapping approach that we previously proposed[34] and efficiently narrowed the locus to 2.45 Mb. Typically, congenic lines are backcrossed for at least 10 generations to remove genetic variation outside of QTL intervals[53]. Here, the genetic background of C57BL/6 substrains is already > 99.99% isogenic and thus, the remote possibility for epistasis is even less likely, especially after just a single generation of backcrossing, let alone the three to eight additional generations of backcrossing that we implemented from N5-N10 generations.

The QTL intervals for OXY locomotion and withdrawal overlapped, suggesting a common underlying genetic basis. This hypothesis is supported by the N6-1 recombinant line (161-183 Mb) which captured a phenotype for OXY locomotion and withdrawal (**Fig.3C,J**). Intriguingly, however, the OXY-responsive allelic effect of J/J for EPM behavior was opposite in N6-1 (decrease in Open Arm Entries; **Fig.3J**) versus F2 mice (increase in Open Arm Entries; **Fig.2G, I**). Nevertheless, the J/J genotype in both cases was the OXY-

responsive allele to alterations in EPM behavior. The source of discrepancy is unknown; however, note that despite the OXY-induced increase in Open Arm Entries (**Fig.2G**) and Open Arm Distance (**Fig.S3G**), mice showed a robust OXY-induced decrease in % Open Arm Time (**Fig.S3H**). Once explanation is that a different experimenter was responsible for N6-1 versus F2 genotyping[54]. Also, previous studies with C57BL/6 have observed either a decrease[55] and an increase in EPM behaviors[56–58] during opioid withdrawal.

One major candidate gene in which knockout affects opioid behavioral sensitivity and withdrawal is *Kcnj9*, which codes for G protein-inwardly Rectifying K+ channel 3 (GIRK3, a.k.a. Kir3.3). Multiple addictive substances acting directly (e.g., morphine) or indirectly through GPCRs to modulate GIRK3, thus unleashing the dopaminergic reward pathway and stimulating acute and reinforcing behaviors[59]. Evidence indicates that morphine activates mu opioid receptors in VTA GABAergic neurons, leading to GIRK3-mediated neuronal inhibition, disinhibition of mesolimbic dopamine neurons, and locomotor activation[60]. *Kcnj9*/GIRK3 (172.32 Mb) lies within the 170.16-172.61 Mb region, has a cis-eQTL that peaked at the behavioral QTL, and shows a decrease in KCNJ9/GIRK3 protein in J/N (**Figs.4,5**). Reduced KCNJ9 protein in J/N is predicted to reduce OXY locomotion and withdrawal, given that GIRK3 is a major effector of mu opioid receptor signaling and is necessary for opioid-induced locomotion[60], opioid antinociception and multiple opioid withdrawal phenotypes[61,62]. Another F2 study between C57BL/6J and 129P3/J mapped a similar distal chromosome 1 locus for antinociception induced by multiple Gi/Go-coupled GPCR drug classes (opioids, alpha-2 adrenergics, cannabinoids); however, when testing *Kcnj9* knockouts, they found no difference in morphine antinociception[63]. A portion of our 2.45-Mb region (172,138,540-172,571,795 bp; mm10) was also identified for withdrawal induced by sedative/hypnotics acting at the GABA-A receptor and *Kcnj9* knockouts showed reduced withdrawal (handling-induced convulsions)[62]. To summarize, *Kcnj9* is a compelling positional and functional candidate gene underlying OXY behavioral sensitivity and withdrawal.

A second positional/functional candidate within the 2.45-Mb region is *Atp1a2* (sodium/potassium-transporting ATPase subunit alpha-2) which has a cis-eQTL that we validated as showing a robust increase in protein in J/N. Atp1a2 codes for a plasma membrane protein enzyme that regulates Na+ and K+ concentrations across the cell membrane, thus influencing the resting potential, depolarization, neurotransmitter release, and excitability. An adaptation in brain dopamine- and norepinephrine Na+/K+ ATPase activity following chronic opioid administration is hypothesized to contribute to changes in neuronal firing underlying opioid dependence[64]. For example, short-term morphine treatment in vivo can stimulate striatal Na+/K+ ATPase activity and inhibit neuronal depolarization via a D2 dopamine receptors and long-term morphine treatment can decrease synaptic protein expression and activity of Na+/K+ ATPase[65] and increase neuronal depolarization through a D1 dopamine receptor-dependent mechanism both through cAMP/PKA-dependent mechanisms and which ultimately depend on mu opioid receptor activation[66,67]. Thus, repeated high-dose OXY could induce neuronal hyperexcitability and depolarization accompanying opioid dependence[68] through an Na+/K+ ATPase-dependent mechanism[69], a physiological effect whose magnitude could depend on genotype-dependent differences in ATP1A2 protein levels. Also, the causal genes underlying the distal

chromosome 1 QTL could be different for acute (e.g., *Kcnj9*) versus chronic (e.g., *Atp1a2*) behavioral effects of OXY or that both genes could contribute to both OXY behaviors.

Although *Rgs7* (regulator of G-protein signaling, 7) is located distal to 170.16-172.61 Mb at 175.06 Mb, we would be remiss if we did not entertain *Rgs7* as a candidate gene for OXY locomotion and withdrawal. RGS proteins (regulators of g-protein signaling) serve as brakes on GPCR signaling and accordingly, *Rgs7* knockouts showed increase morphine locomotion, reward, reinforcement, and withdrawal[70]. Consistent with these observations, we found a non-significant increase in RGS7 protein in the J/N genotype ($p = 0.08$) that showed decreased OXY locomotion and withdrawal (**Figs.3-5**). Although *Rgs7* lies outside of the 2.45-Mb region, it is possible that one or more regulatory variants within the 2.45 Mb locus could modulate *Rgs7* expression[71].

We identified a second medial chromosome 5 QTL for OXY withdrawal that overlapped with the *Gabra2*-containing QTL[36] that we identified and validated for methamphetamine stimulant sensitivity[23]. *Gabra2* is a compelling candidate gene for anxiety-like behavior during opioid withdrawal, given its importance in the anxiogenic and anxiolytic properties benzodiazepine-site drugs, alcohol dependence, and polydrug misuse[50,52]. GABRA2-linked variants are associated with a disrupted connectome of reward circuits and cognitive deficits in heroin users[72] as well as polysubstance use and alcohol dependence[73]. The Gabra2 eQTL is mediated by a single intronic nucleotide deletion near a splice site in B6J that causes a loss-of-function (expression) at the mRNA and protein levels[36]. Thus, *Gabra2* is a high priority candidate gene underlying anxiety-like OXY withdrawal on the EPM. Nevertheless, the peak marker for the behavioral QTL (rs33209545; 59.83 Mb) was a bit more proximally located versus *Gabra2* (71 Mb) and thus we also considered cis-eQTLs showing peak linkage with rs33209545 (**Table S5**). Candidate genes with peak cis-eQTLs at rs33209545 include *Cpeb2*, *N4bp2*, *Gabra4*, *Pdgfra*, and *Clock*. A human linkage scan of comorbid dependence on multiple substances, including opioids, identified significant linkage with a locus containing *GABRA4*, *GABRB1*, and *CLOCK*[74]. Furthermore, clock genes have long been implicated in addiction traits[75], including opioid withdrawal[76–81].

While there are many strengths to this study (fine mapping, functional analysis at RNA and protein level), there are some limitations. First, despite our most valiant effort, we were unable to resolve the 2.45-Mb locus any further, due to reasons described above. Second, we only conducted cis-eQTL analysis from one tissue (striatum) and thus, there could be additional cis-eQTLs in other brain regions. We chose striatum for practical reasons as it is large and readily amenable to RNA-seq analysis and it is rich in mu opioid receptors that contribute directly to opioid-induced locomotor sensitivity[82]. Third, while we obtained functional evidence at the gene level for causal sources of behavior, we do not have any obvious candidate causal quantitative trait variants. At the moment, future validation studies of candidate genes will require modulation of gene expression (e.g., virally-mediated) rather than germline gene editing.

In summary, we extended C57BL/6 substrain differences to include opioid behavioral sensitivity and withdrawal and identified strong candidate genes on distal chromosome 1 (Kcnj9, Atp1a2) through a novel positional cloning strategy unique to reduced complexity crosses combined with multi-level functional analyses.

We also identified a chromosome 5 for opioid withdrawal, where Gabra2 is a likely a compelling candidate gene. Given that C57BL/6 is the most widely used mouse strain in biomedical research and given the huge focus of preclinical addiction research on opioids (which largely employs C57BL/6 mice), investigators should be aware of these genetic sources of variance in opioid behaviors as they ponder which C57BL/6 substrain to use in their opioid studies.

DATA AVAILABILITY STATEMENT

Data are available and will be provided by the corresponding author upon request.

FUNDING

U01DA055299, U01DA050243, T32DA055553, R03DA038287, R21DA038738

AUTHOR CONTRIBUTIONS

L.R.G.: Data collection, analysis, and writing of manuscript; B.M.B: Data analysis and writing of manuscript Y.A.: Data analysis; J.A.B.: Data analysis and writing of the manuscript; J.C. K.: Data collection and analysis; E.J.Y.: Data collection and analysis; S.L.K.: Data collection and analysis; E.R.R.: Data collection and analysis; D.F.J.: Data analysis; A.M.L.: Data collection and analysis; K.P.L.: Data collection; J.A.S.: Data collection; T.A.D.: Data collection; S.B.C.: Data collection; N.Y.: Data analysis; M.T.F.: Data analysis; W.E.J.: Data analysis; M.K.M.: Data collection, analysis, and writing of the manuscript

COMPETING INTERESTS

The authors have nothing to disclose.

FIGURE LEGENDS

Figure 1. OXY-induced locomotor activity and conditioned place preference in B6J vs. B6NJ substrains. (A): Schematic of OXY-CPP protocol. D=Day. **(B):** Dose-dependent increase in OXY-induced locomotor activity (m).**p<0.01 vs. 0 mg/kg. ****p<0.05 vs. all other doses. **(C):** Time course of D2 OXY-induced locomotor activity. **p<0.0001 (Substrain effect). **(D):** Dose-dependent increase in OXY-induced locomotor activity (m) in 5-min bins over 30 min. *p<0.05 (0.6125 vs. 1.25 mg/kg). ***p < 0.001 (1.25 vs. 0 mg/kg). ****p<0.0001 (5 vs. 0 mg/kg and vs. 0.6125 mg/kg). **(E):** Time course of D4 OXY-induced locomotor activity (m) in 5-min bins over 30 min. **p<0.0001 (Substrain effect). **(F,G):** Dose-response for drug-free OXY-CPP on D8 (D8-D1, s) and state-dependent OXY-CPP on D9 (D9-D1, s). *p<0.05 (0.6125 vs. 0 mg/kg); **p<0.01 (0.6125 vs. 0 mg/kg); **p<0.01 (5 vs. 0 mg/kg). ***p<0.001 (1.25 vs. 0 mg/kg). ****p<0.0001 (5 vs 0 mg/kg).

Figure 2. QTLs on chromosomes 1 and 5 underlying OXY locomotion and spontaneous withdrawal. (A): Summary of QTL results for six OXY-induced locomotor traits and three EPM-related traits during spontaneous OXY withdrawal. **(B):** Genome-wide plot of OXY-induced locomotor behaviors (Distance, Spins, Rotations) on D2 and D4 following 1.25 mg/kg OXY (i.p.). **(C):** Chromosome 1 QTL plot for D2 and D4 OXY behaviors. **(D):** Chromosome 1 effect plot for D2 OXY Distance. **(E):** Genome-wide QTL plot of EPM behaviors during spontaneous OXY withdrawal behaviors. **(F):** Chromosome 1 QTL plot for EPM behaviors. **(G):** Chromosome 1 effect plot at peak-associated marker for Open Arm Entries (#). **(H):** Chromosome 5 plot for Open Arm Entries (#)**. (I):** Chromosome 5 effect plot at peak-associated marker for Open Arm Entries.

Figure 3: Capture of the distal chromosome 1 QTL for OXY locomotion and withdrawal in the N6-1 recombinant line. (A): Schematic of the N6-1 recombinant interval spanning 163-181 Mb. Blue ticks on the x-axis indicate marker location (Mb). Burgundy color = homozygous J/J. Mauve color = heterozygous J/N. White color = region of uncertainty for recombination breakpoint. **(B):** Significant decrease in D1 distance in the J/N vs. J/J genotype. **(C):** Significant reduction in D2 OXY distance in the J/N vs. J/J Genotype (****p<0.0001). **(D):** Time course of D4 OXY distance in 5-min bins over 30 min. **(E):** D4 OXY distance (Treatment: ****p < 0.0001). **(F):** Time course of D4 OXY distance. **(G):** D8 Drug-free OXY-CPP (Treatment: **p<0.01). **(H):** D9 State-dependent OXY-CPP. (Treatment: *p<0.05). **(I-K):** EPM behaviors during spontaneous OXY withdrawal. Treatment effect (panel J, Open Arm Entries: **p<0.01, OXY<SAL). Significant reduction in Open Arm Entries in OXY J/J vs. SAL J/J (panel J: *p<0.05).

Figure 4. Positional cloning of a 2.45 Mb region on distal chromosome 1 underlying OXY locomotor traits in recombinant lines backcrossed to B6J. (A): Schematic of the eight congenic lines that were used to deduce a 2.45 Mb region spanning 170.16-172.61 Mb. Blue ticks on the x-axis indicate marker location (Mb). Burgundy color: homozygous J/J genotype. Mauve color: heterozygous J/N genotype. White color =

region of uncertainty for recombination breakpoint. "+" = captured the QTL for reduced D2 OXY distance. "-" = failed to capture the QTL for reduced D2 OXY distance. **(B-D, vertically):** D1 Distance, D1 Rotations, and D1 Spins following SAL (i.p.) in eight recombinant lines. **p<0.00625. **(E-G, vertically):** D2 Distance, D2 Rotations, and D2 Spines following OXY (1.25 mg/kg, i.p.). ****p<0.0001 (N6-1 line, D2 Distance, D2 Rotations: J/N vs. J/J). ***p<0.001 (N6-1, D2 Spins: J'N vs. J/J and also N9-8, D2 Distance, D2 Rotations, D2 Spins: J/N vs. J/J).

Figure 5. Protein analysis of striatal cis-eQTL transcripts within or distal to the fine-mapped 2.45 Mb region (chromosome 1: 170.16-172.61 Mb) for D2 OXY behavioral sensitivity. (A): Striatal cis-eQTL transcripts within the 170.16-172.61 Mb interval (Pcprl1, Atp1a2, Kcnj9, and Igsf9) and also cis-eQTL transcripts just distal to this region (Cadm3, Aim2, and Rgs7). See **Supplementary Table 4** for full list of cis-eQTLs showing a peak association with rs51237371 (181.32 Mb). (B-H): Immunoblot analysis of proteins coded by candidate genes within the 2.45 Mb region on distal chromosome 1. ****p<0.0001 (panel C: ATP1A2). *p<0.05 (panel D: KCNJ9).

FIGURE 1

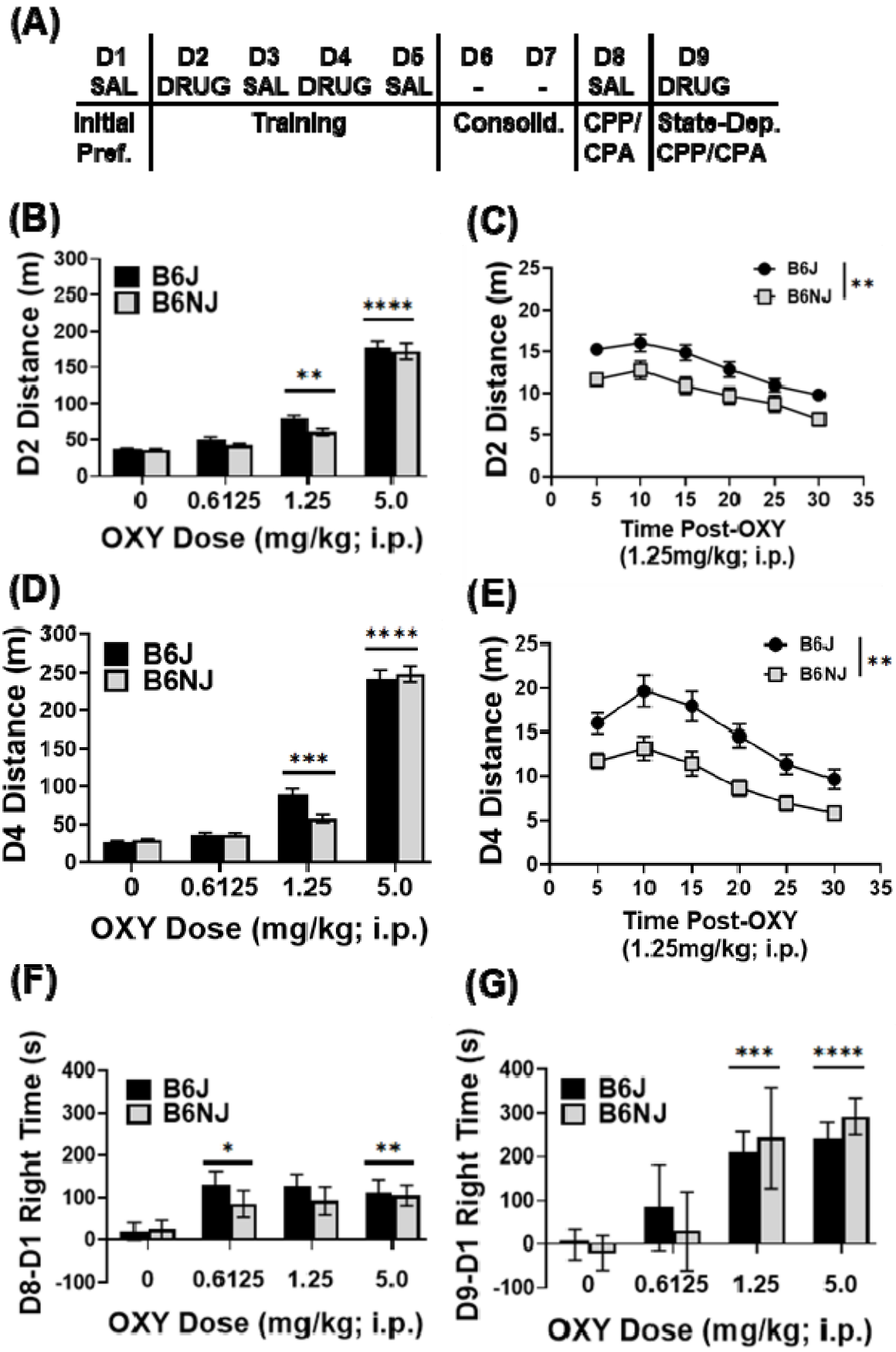

FIGURE 2

(A) QTL Summary Table

Phenotype	Chr	Pos (cM)	LOD	pval	Bayesint (cM)	1.5 LOD (cM)	% var	Expanded to markers (Mb)
D2.Distance (cm)	1	62.326	6.10	0.003	76.33 - 84.66	72.42 - 84.66	6.66	163.13 Mb-181.32 Mb (rs6341208-rs51237371)
D2 Spins (#)	1	61.326	9.11	p<0.001	76.33 - 84.66	73.33 - 84.66	9.43	163.13 Mb-181.32 Mb (rs6341208-rs51237371)
D2 Rotations (#)	1	62.326	9.94	p<0.001	76.33 - 84.66	76.33 - 84.66	11.96	163.13 Mb-181.32 Mb (rs6341208-rs51237371)
D4 Distance (cm)	1	62.326	2.30	0.101	76.33 - 84.66	73.33 - 84.66	6.84	163.13 Mb-181.32 Mb (rs6341208-rs51237371)
D4 Spins (#)	1	62.326	5.66	0.021	76.33 - 84.66	73.33 - 84.66	7.32	163.13 Mb-181.32 Mb (rs6341208-rs51237371)
D4 Rotations (#)	1	61.326	7.30	0.001	76.33 - 84.66	72.43 - 84.66		163.13 Mb-181.32 Mb (rs6341208-rs51237371)
EPM: Open Arm Entries (#)	1	64.33	5.69	0.006	76.33 - 84.66	71.33 - 84.66	10.06	116.04 Mb-181.32 Mb (rs32160662-rs512377371)
EPM: Open Arm Distance (cm)	1	76.33	5.06	0.016	67.33 - 84.66	61.33 - 84.66	6.93	116.04 Mb-181.32 Mb (rs32160662-rs512377371)
EPM: Open Arm Time (%)	1	77.33	5.13	0.016	82.33 - 84.66	66.33 - 84.66	7.36	116.04 Mb-181.32 Mb (rs32160662-rs512377371)
EPM: Open Arm Entries (#)	5	31.76	5.04	0.016	27.37 - 43.37	26.37 - 46.37	8.86	40.76 Mb-131.64 Mb (rs33608771-rs3719791)

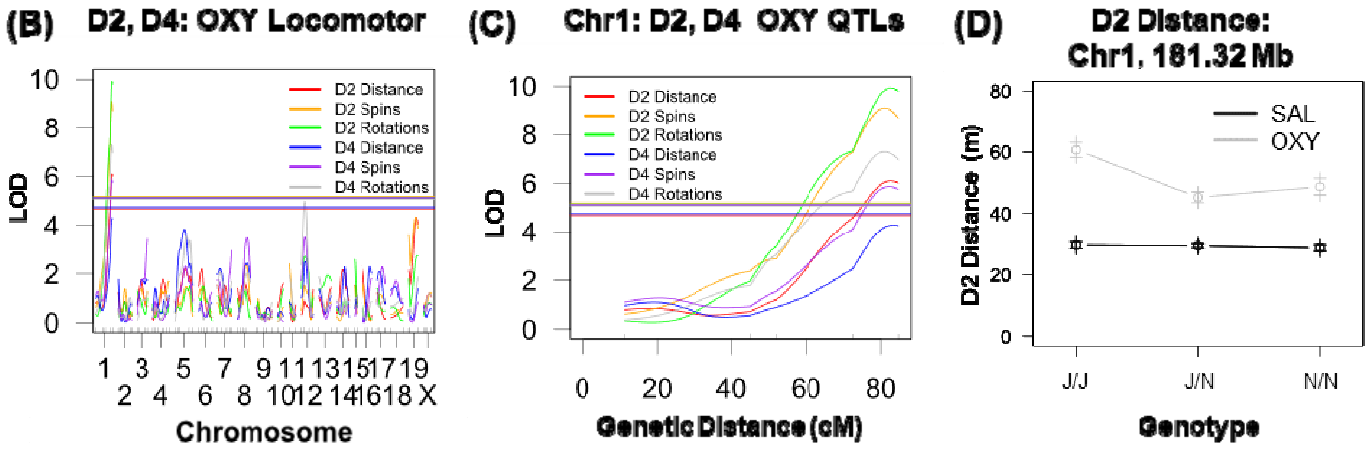

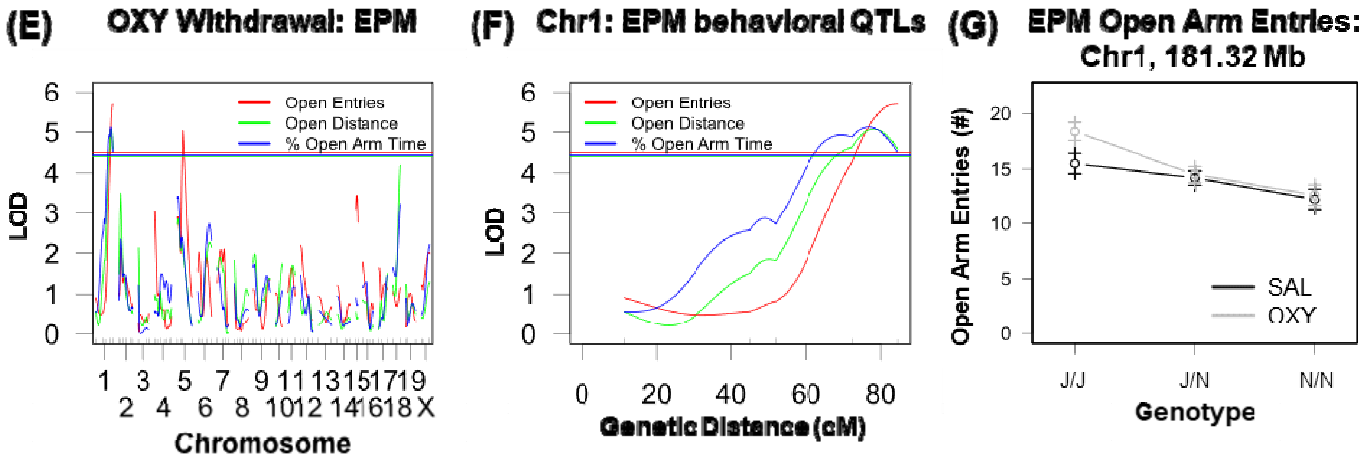

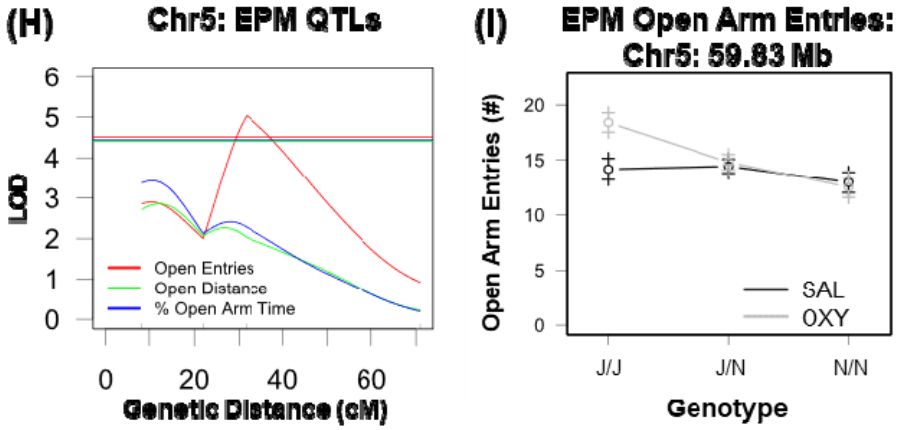

FIGURE 3

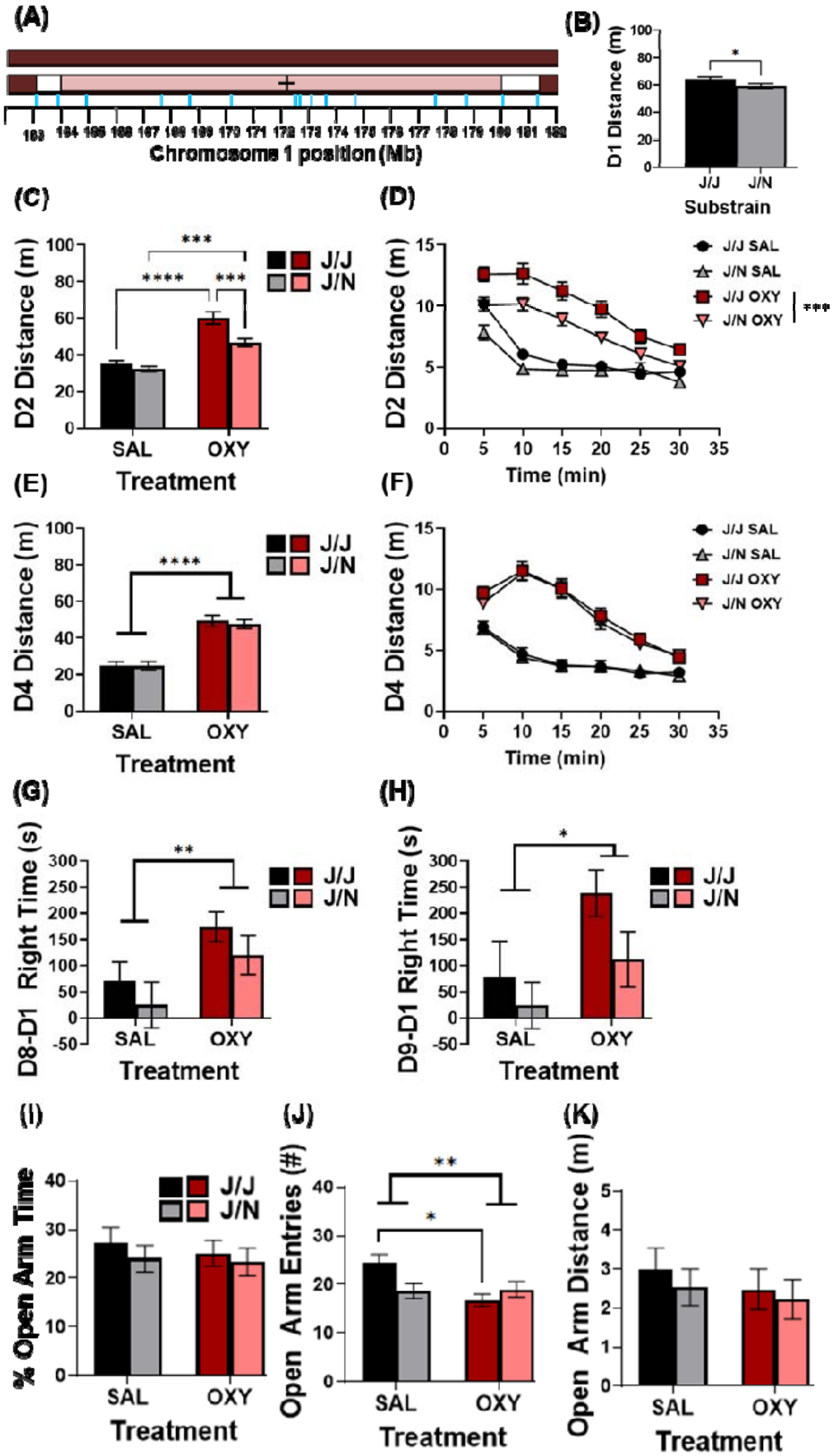

FIGURE 4

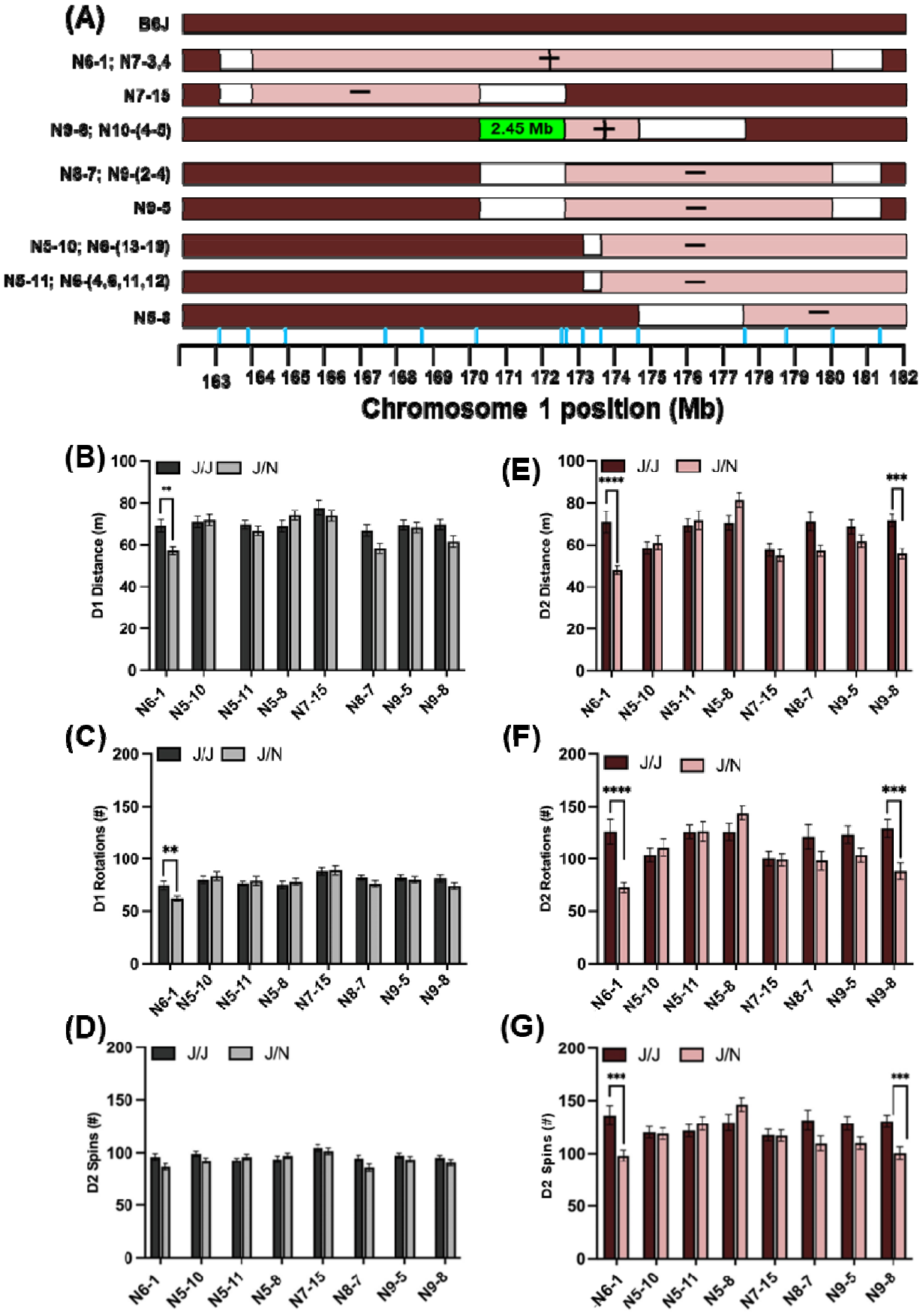

FIGURE 5

(A)

geneID	chr	start	end	AvExp	F	P.Value	adj.P.Val
Pcp4l1	1	171173262	171196268	8.64	4.81	4.17E-06	0.00023
Ncstn	1	172066013	172082795	5.72	-3.48	0.00068	0.01021
Atp1a2	1	172271709	172298064	9.74	-4.03	9.55E-05	0.00233
Kcnj9	1	172320501	172329318	6.74	-3.34	0.00109	0.01439
Igsf9	1	172481788	172498878	3.78	3.10	0.00241	0.02547
Cadm3	1	173333258	173367895	8.63	-4.43	2.05E-05	0.00075
Aim2	1	173350879	173466040	1.84	-3.16	0.00199	0.02223
Rgs7	1	175059087	175492500	4.93	-3.25	0.00147	0.01795

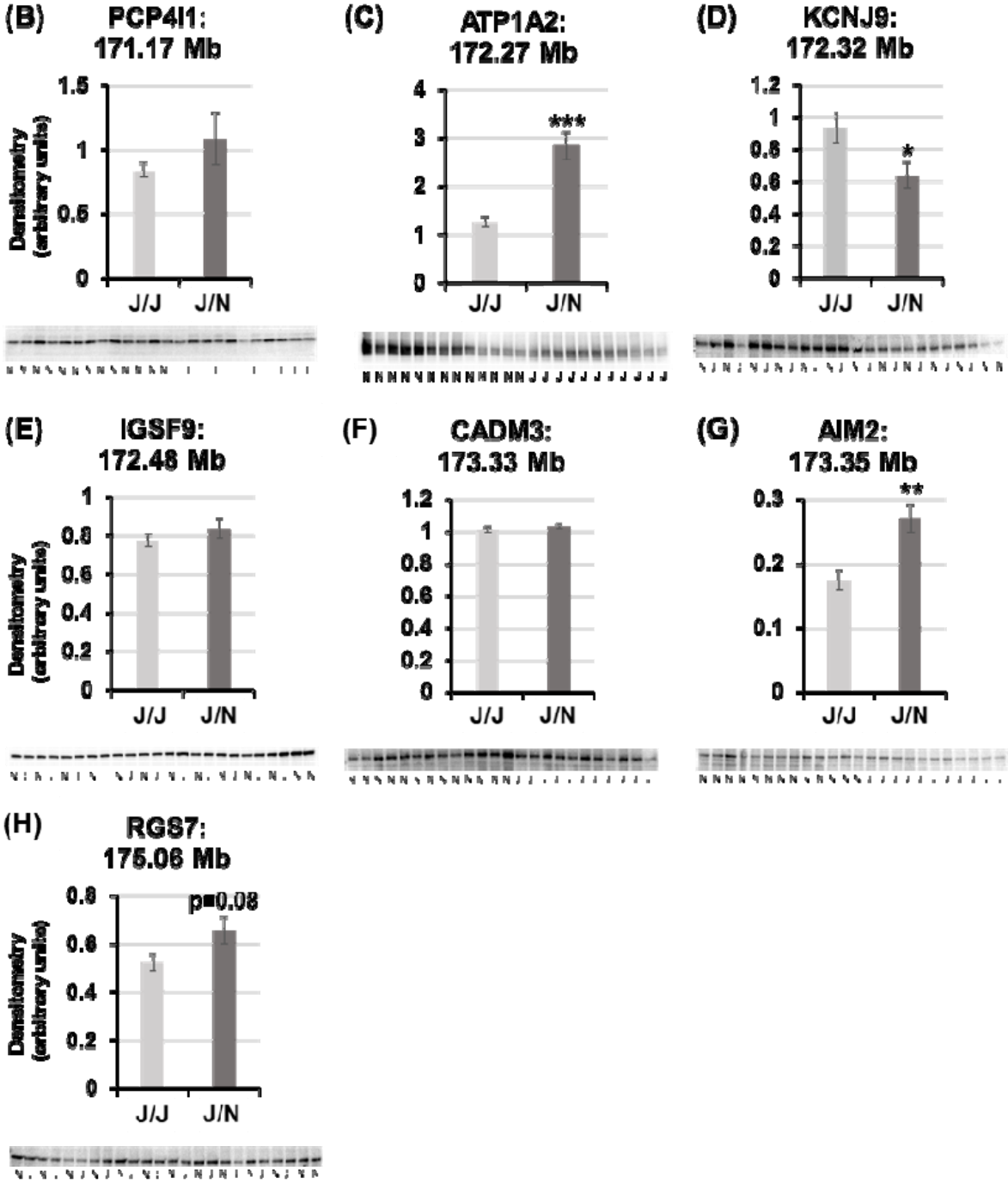

REFERENCES

1 Kibaly C, Alderete JA, Liu SH, Nasef HS, Law P-Y, Evans CJ *et al.* Oxycodone in the Opioid Epidemic: High 'Liking', 'Wanting', and Abuse Liability. *Cell Mol Neurobiol* 2021; **41**: 899–926.

2 Cicero TJ, Ellis MS. Abuse-Deterrent Formulations and the Prescription Opioid Abuse Epidemic in the United States: Lessons Learned From OxyContin. *JAMA Psychiatry* 2015; **72**: 424–430.

3 Perdue T, Carlson R, Daniulaityte R, Silverstein SM, Bluthenthal RN, Valdez A *et al.* Characterizing prescription opioid, heroin, and fentanyl initiation trajectories: A qualitative study. *Soc Sci Med* 2024; **340**: 116441.

4 Ducci F, Goldman D. The genetic basis of addictive disorders. *PsychiatrClinNorth Am* 2012; **35**: 495–519.

5 Ho MK, Goldman D, Heinz A, Kaprio J, Kreek MJ, Li MD *et al.* Breaking barriers in the genomics and pharmacogenetics of drug addiction. *ClinPharmacolTher* 2010; **88**: 779–791.

6 Gelernter J, Polimanti R. Genetics of substance use disorders in the era of big data. *Nat Rev Genet* 2021; **22**: 712–729.

7 Gaddis N, Mathur R, Marks J, Zhou L, Quach B, Waldrop A *et al.* Multi-trait genome-wide association study of opioid addiction: OPRM1 and beyond. *Sci Rep* 2022; **12**: 16873.

8 Deak JD, Zhou H, Galimberti M, Levey DF, Wendt FR, Sanchez-Roige S *et al.* Genome-wide association study in individuals of European and African ancestry and multi-trait analysis of opioid use disorder identifies 19 independent genome-wide significant risk loci. *Mol Psychiatry* 2022; **27**: 3970–3979.

9 Wise RA, Bozarth MA. A psychomotor stimulant theory of addiction. *Psychological review* 1987; **94**: 469–92.

10 Di Chiara G, Imperato A. Drugs abused by humans preferentially increase synaptic dopamine concentrations in the mesolimbic system of freely moving rats. *Proceedings of the National Academy of Sciences of the United States of America* 1988; **85**: 5274–8.

11 Adinoff B. Neurobiologic processes in drug reward and addiction. *Harv Rev Psychiatry* 2004; **12**: 305–320.

12 Bryant CD, Parker CC, Zhou L, Olker C, Chandrasekaran RY, Wager TT *et al.* Csnk1e is a genetic regulator of sensitivity to psychostimulants and opioids. *Neuropsychopharmacology* 2012; **37**: 1026–1035.

13 Bryant CD, Healy AF, Ruan QT, Coehlo MA, Lustig E, Yazdani N *et al.* Sex-dependent effects of an Hnrnph1 mutation on fentanyl addiction-relevant behaviors but not antinociception in mice. *Genes Brain Behav* 2021; **20**: e12711.

14 Yazdani N, Parker CC, Shen Y, Reed ER, Guido MA, Kole LA *et al.* Hnrnph1 Is A Quantitative Trait Gene for Methamphetamine Sensitivity. *PLoS Genet* 2015; **11**: e1005713.

15 Goldberg LR, Kirkpatrick SL, Yazdani N, Luttik KP, Lacki OA, Babbs RK *et al.* Casein kinase 1-epsilon deletion increases mu opioid receptor-dependent behaviors and binge eating1. *Genes Brain Behav* 2017; **16**: 725–738.

16 Ruan QT, Yazdani N, Blum BC, Beierle JA, Lin W, Coelho MA *et al.* A Mutation in Hnrnph1 That Decreases Methamphetamine-Induced Reinforcement, Reward, and Dopamine Release and Increases Synaptosomal hnRNP H and Mitochondrial Proteins. *J Neurosci* 2020; **40**: 107–130.

17 Jordan CJ, Xi Z-X. Identification of the Risk Genes Associated With Vulnerability to Addiction: Major Findings From Transgenic Animals. *Front Neurosci* 2021; **15**: 811192.

18 Bryant CD, Zhang NN, Sokoloff G, Fanselow MS, Ennes HS, Palmer AA *et al.* Behavioral differences among C57BL/6 substrains: implications for transgenic and knockout studies. *JNeurogenet* 2008; **22**: 315–331.

19 Mulligan MK, Ponomarev I, Boehm SL 2nd, Owen JA, Levin PS, Berman AE *et al.* Alcohol trait and transcriptional genomic analysis of C57BL/6 substrains. *Genes Brain Behav* 2008; **7**: 677–689.

20 Warden AS, DaCosta A, Mason S, Blednov YA, Mayfield RD, Harris RA. Inbred Substrain Differences Influence Neuroimmune Response and Drinking Behavior. *Alcohol Clin Exp Res* 2020; **44**: 1760–1768.

21 Jimenez Chavez CL, Bryant CD, Munn-Chernoff MA, Szumlinski KK. Selective Inhibition of PDE4B Reduces Binge Drinking in Two C57BL/6 Substrains. *Int J Mol Sci* 2021; **22**. doi:10.3390/ijms22115443.

22 Kumar V, Kim K, Joseph C, Kourrich S, Yoo SH, Huang HC *et al.* C57BL/6N mutation in Cytoplasmic FMRP interacting protein 2 regulates cocaine response. *Science* 2013; **342**: 1508–1512.

23 Goldberg LR, Yao EJ, Kelliher JC, Reed ER, Wu Cox J, Parks C *et al.* A quantitative trait variant in Gabra2 underlies increased methamphetamine stimulant sensitivity. *Genes Brain Behav* 2021; **20**: e12774.

24 Akinola LS, Mckiver B, Toma W, Zhu AZX, Tyndale RF, Kumar V *et al.* C57BL/6 Substrain Differences in Pharmacological Effects after Acute and Repeated Nicotine Administration. *Brain Sci* 2019; **9**. doi:10.3390/brainsci9100244.

25 Kirkpatrick SL, Bryant CD. Behavioral architecture of opioid reward and aversion in C57BL/6 substrains. *FrontBehavNeurosci* 2015; **8**: 450.

26 Kirkpatrick SL, Goldberg LR, Yazdani N, Babbs RK, Wu J, Reed ER *et al.* Cytoplasmic FMR1-Interacting Protein 2 Is a Major Genetic Factor Underlying Binge Eating. *BiolPsychiatry* 2017; **81**: 757–769.

27 Babbs RK, Beierle JA, Yao EJ, Kelliher JC, Medeiros AR, Anandakumar J *et al.* The effect of the demyelinating agent cuprizone on binge-like eating of sweetened palatable food in female and male C57BL/6 substrains. *Appetite* 2020; **150**: 104678.

28 Matsuo N, Takao K, Nakanishi K, Yamasaki N, Tanda K, Miyakawa T. Behavioral profiles of three C57BL/6 substrains. *FrontBehavNeurosci* 2010; **4**: 29.

29 Simon MM, Greenaway S, White JK, Fuchs H, Gailus-Durner V, Sorg T *et al.* A comparative phenotypic and genomic analysis of C57BL/6J and C57BL/6N mouse strains. *Genome Biol* 2013; **14**: R82.

30 Keane TM, Goodstadt L, Danecek P, White MA, Wong K, Yalcin B *et al.* Mouse genomic variation and its effect on phenotypes and gene regulation. *Nature* 2011; **477**: 289–294.

31 Yalcin B, Wong K, Agam A, Goodson M, Keane TM, Gan X *et al.* Sequence-based characterization of structural variation in the mouse genome. *Nature* 2011; **477**: 326–329.

32 Mortazavi M, Ren Y, Saini S, Antaki D, St Pierre CL, Williams A *et al.* SNPs, short tandem repeats, and structural variants are responsible for differential gene expression across C57BL/6 and C57BL/10 substrains. *Cell Genom* 2022; **2**: 100102.

33 Ferraj A, Audano PA, Balachandran P, Czechanski A, Flores JI, Radecki AA *et al.* Resolution of structural variation in diverse mouse genomes reveals chromatin remodeling due to transposable elements. *Cell Genom* 2023; **3**: 100291.

34 Bryant CD, Ferris MT De Villena,FPM, Damaj MI, Kumar V, Mulligan MK. Reduced complexity cross design for behavioral genetics. In: Gerlai RT (ed). *Molecular-Genetic and Statistical Techniques for Behavioral and Neural Research*. 2018, pp 165–190.

35 Bryant CD, Smith DJ, Kantak KM, Nowak TS, Williams RW, Damaj MI *et al.* Facilitating Complex Trait Analysis via Reduced Complexity Crosses. *Trends Genet* 2020; **36**: 549–562.

36 Mulligan MK, Abreo T, Neuner SM, Parks C, Watkins CE, Houseal MT *et al.* Identification of a functional non-coding variant in the GABAA receptor α2 subunit of the C57BL/6J mouse reference genome: Major implications for neuroscience research. *Frontiers in Genetics* 2019; : 540211.

37 Goldberg LR, Yao EJ, Kelliher JC, Reed ER, Wu Cox J, Parks C *et al.* A quantitative trait variant in Gabra2 underlies increased methamphetamine stimulant sensitivity. *BioRxiv* 2021; **450337**.

38 Harkness JH, Shi X, Janowsky A, Phillips TJ. Trace Amine-Associated Receptor 1 Regulation of Methamphetamine Intake and Related Traits. *Neuropsychopharmacology* 2015; **40**: 2175–2184.

39 Shi X, Walter NA, Harkness JH, Neve KA, Williams RW, Lu L *et al.* Genetic Polymorphisms Affect Mouse and Human Trace Amine-Associated Receptor 1 Function. *PLoS One* 2016; **11**: e0152581.

40 Miner NB, Elmore JS, Baumann MH, Phillips TJ, Janowsky A. Trace amine-associated receptor 1 regulation of methamphetamine-induced neurotoxicity. *Neurotoxicology* 2017; **63**: 57–69.

41 Reed C, Baba H, Zhu Z, Erk J, Mootz JR, Varra NM *et al.* A Spontaneous Mutation in Taar1 Impacts Methamphetamine-Related Traits Exclusively in DBA/2 Mice from a Single Vendor. *Front Pharmacol* 2017; **8**: 993.

42 Phillips TJ, Roy T, Aldrich SJ, Baba H, Erk J, Mootz JRK *et al.* Confirmation of a Causal Taar1 Allelic Variant in Addiction-Relevant Methamphetamine Behaviors. *Front Psychiatry* 2021; **12**: 725839.

43 Beierle JA, Yao EJ, Goldstein SI, Lynch WB, Scotellaro JL, Shah AA *et al.* Zhx2 Is a Candidate Gene Underlying Oxymorphone Metabolite Brain Concentration Associated with State-Dependent Oxycodone Reward. *J Pharmacol Exp Ther* 2022; **382**: 167–180.

44 Beierle JA, Yao EJ, Goldstein SI, Scotellaro JL, Sena KD, Linnertz CA *et al.* Genetic basis of thermal nociceptive sensitivity and brain weight in a BALB/c reduced complexity cross. *Mol Pain* 2022; **18**: 17448069221079540.

45 Bryant CD, Bagdas D, Goldberg LR, Khalefa T, Reed ER, Kirkpatrick SL *et al.* C57BL/6 substrain differences in inflammatory and neuropathic nociception and genetic mapping of a major quantitative trait locus underlying acute thermal nociception. *Mol Pain* 2019; : 1744806918825046.

46 Hegmann JP, Possidente B. Estimating genetic correlations from inbred strains. *BehavGenet* 1981; **11**: 103–114.

47 Schulteis G, Yackey M, Risbrough V, Koob GF. Anxiogenic-like effects of spontaneous and naloxone-precipitated opiate withdrawal in the elevated plus-maze. *Pharmacol Biochem Behav* 1998; **60**: 727–731.

48 Hawkins NA, Nomura T, Duarte S, Barse L, Williams RW, Homanics GE *et al.* Gabra2 is a genetic modifier of Dravet syndrome in mice. *Mamm Genome* 2021; **32**: 350–363.

49 Yu W, Mulligan MK, Williams RW, Meisler MH. Correction of the hypomorphic Gabra2 splice site variant in mouse strain C57BL/6J modifies the severity of Scn8a encephalopathy. *HGG Adv* 2022; **3**: 100064.

50 Engin E, Liu J, Rudolph U. α2-containing GABA(A) receptors: a target for the development of novel treatment strategies for CNS disorders. *Pharmacol Ther* 2012; **136**: 142–152.

51 Yao EJ, Babbs RK, Kelliher JC, Luttik KP, Borrelli KN, Damaj MI *et al.* Systems genetic analysis of binge-like eating in a C57BL/6J x DBA/2J-F2 cross. *Genes Brain Behav* 2021; : e12751.

52 Löw K, Crestani F, Keist R, Benke D, Brünig I, Benson JA *et al.* Molecular and neuronal substrate for the selective attenuation of anxiety. *Science* 2000; **290**: 131–134.

53 Davis RC, Schadt EE, Smith DJ, Hsieh EWY, Cervino ACL, van Nas A *et al.* A genome-wide set of congenic mouse strains derived from DBA/2J on a C57BL/6J background. *Genomics* 2005; **86**: 259–270.

54 Chesler EJ, Wilson SG, Lariviere WR, Rodriguez-Zas SL, Mogil JS. Identification and ranking of genetic and laboratory environment factors influencing a behavioral trait, thermal nociception, via computational analysis of a large data archive. *Neurosci Biobehav Rev* 2002; **26**: 907–923.

55 Ozdemir D, Allain F, Kieffer BL, Darcq E. Advances in the characterization of negative affect caused by acute and protracted opioid withdrawal using animal models. *Neuropharmacology* 2023; **232**: 109524.

56 Hodgson SR, Hofford RS, Norris CJ, Eitan S. Increased elevated plus maze open-arm time in mice during naloxone-precipitated morphine withdrawal. *BehavPharmacol* 2008; **19**: 805–811.

57 Buckman SG, Hodgson SR, Hofford RS, Eitan S. Increased elevated plus maze open-arm time in mice during spontaneous morphine withdrawal. *BehavBrain Res* 2009; **197**: 454–456.

58 Hofford RS, Hodgson SR, Roberts KW, Bryant CD, Evans CJ, Eitan S. Extracellular signal-regulated kinase activation in the amygdala mediates elevated plus maze behavior during opioid withdrawal. *BehavPharmacol* 2009; **20**: 576–583.

59 Rifkin RA, Moss SJ, Slesinger PA. G Protein-Gated Potassium Channels: A Link to Drug Addiction. *Trends Pharmacol Sci* 2017; **38**: 378–392.

60 Kotecki L, Hearing M, McCall NM, Marron Fernandez de Velasco E, Pravetoni M, Arora D *et al.* GIRK Channels Modulate Opioid-Induced Motor Activity in a Cell Type- and Subunit-Dependent Manner. *J Neurosci* 2015; **35**: 7131–7142.

61 Cruz HG, Berton F, Sollini M, Blanchet C, Pravetoni M, Wickman K *et al.* Absence and rescue of morphine withdrawal in GIRK/Kir3 knock-out mice. *J Neurosci* 2008; **28**: 4069–4077.

62 Kozell LB, Walter NAR, Milner LC, Wickman K, Buck KJ. Mapping a barbiturate withdrawal locus to a 0.44 Mb interval and analysis of a novel null mutant identify a role for Kcnj9 (GIRK3) in withdrawal from pentobarbital, zolpidem, and ethanol. *J Neurosci* 2009; **29**: 11662–11673.

63 Smith SB, Marker CL, Perry C, Liao G, Sotocinal SG, Austin J-S *et al.* Quantitative trait locus and computational mapping identifies Kcnj9 (GIRK3) as a candidate gene affecting analgesia from multiple drug classes. *Pharmacogenet Genomics* 2008; **18**: 231–241.

64 Desaiah D, Ho IK. Effects of acute and continuous morphine administration on catecholamine-sensitive adenosine triphosphatase in mouse brain. *J Pharmacol Exp Ther* 1979; **208**: 80–85.

65 Prokai L, Zharikova AD, Stevens SM. Effect of chronic morphine exposure on the synaptic plasma-membrane subproteome of rats: a quantitative protein profiling study based on isotope-coded affinity tags and liquid chromatography/mass spectrometry. *J Mass Spectrom* 2005; **40**: 169–175.

66 Wu Z-Q, Li M, Chen J, Chi Z-Q, Liu J-G. Involvement of cAMP/cAMP-dependent protein kinase signaling pathway in regulation of Na+,K+-ATPase upon activation of opioid receptors by morphine. *Mol Pharmacol* 2006; **69**: 866–876.

67 Wu Z-Q, Chen J, Chi Z-Q, Liu J-G. Involvement of dopamine system in regulation of Na+,K+-ATPase in the striatum upon activation of opioid receptors by morphine. *Mol Pharmacol* 2007; **71**: 519–530.

68 Kong JQ, Meng J, Biser PS, Fleming WW, Taylor DA. Cellular depolarization of neurons in the locus ceruleus region of the guinea pig associated with the development of tolerance to opioids. *J Pharmacol Exp Ther* 2001; **298**: 909–916.

69 Kong JQ, Leedham JA, Taylor DA, Fleming WW. Evidence that tolerance and dependence of guinea pig myenteric neurons to opioids is a function of altered electrogenic sodium-potassium pumping. *J Pharmacol Exp Ther* 1997; **280**: 593–599.

70 Sutton LP, Ostrovskaya O, Dao M, Xie K, Orlandi C, Smith R *et al.* Regulator of G-Protein Signaling 7 Regulates Reward Behavior by Controlling Opioid Signaling in the Striatum. *BiolPsychiatry* 2016; **80**: 235–245.

71 Smemo S, Tena JJ, Kim K-H, Gamazon ER, Sakabe NJ, Gómez-Marín C *et al.* Obesity-associated variants within FTO form long-range functional connections with IRX3. *Nature* 2014; **507**: 371–375.

72 Sun Y, Zhang Y, Zhang D, Chang S, Jing R, Yue W *et al.* GABRA2 rs279858-linked variants are associated with disrupted structural connectome of reward circuits in heroin abusers. *Transl Psychiatry* 2018; **8**: 1–10.

73 Nudmamud-Thanoi S, Veerasakul S, Thanoi S. Pharmacogenetics of drug dependence: Polymorphisms of genes involved in GABA neurotransmission. *Neurosci Lett* 2020; **726**: 134463.

74 Yang B-Z, Han S, Kranzler HR, Farrer LA, Elston RC, Gelernter J. Autosomal linkage scan for loci predisposing to comorbid dependence on multiple substances. *Am J Med Genet B Neuropsychiatr Genet* 2012; **159B**: 361–369.

75 Forde LA, Kalsi G. Addiction and the Role of Circadian Genes. *J Stud Alcohol Drugs* 2017; **78**: 645–653.

76 Wang X, Wang Y, Xin H, Liu Y, Wang Y, Zheng H *et al.* Altered expression of circadian clock gene, mPer1, in mouse brain and kidney under morphine dependence and withdrawal. *J Circadian Rhythms* 2006; **4**: 9.

77 Li S, Liu L, Jiang W, Lu L. Morphine withdrawal produces circadian rhythm alterations of clock genes in mesolimbic brain areas and peripheral blood mononuclear cells in rats. *J Neurochem* 2009; **109**: 1668–1679.

78 Perreau-Lenz S, Sanchis-Segura C, Leonardi-Essmann F, Schneider M, Spanagel R. Development of morphine-induced tolerance and withdrawal: involvement of the clock gene mPer2. *Eur Neuropsychopharmacol* 2010; **20**: 509–517.

79 Hood S, Cassidy P, Mathewson S, Stewart J, Amir S. Daily morphine injection and withdrawal disrupt 24-h wheel running and PERIOD2 expression patterns in the rat limbic forebrain. *Neuroscience* 2011; **186**: 65–75.

80 Roy K, Bhattacharyya P, Deb I. Naloxone precipitated morphine withdrawal and clock genes expression in striatum: A comparative study in three different protocols for the development of morphine dependence. *Neurosci Lett* 2018; **685**: 24–29.

81 Rahmati-Dehkordi F, Ghaemi-Jandabi M, Garmabi B, Semnanian S, Azizi H. Circadian rhythm influences naloxone induced morphine withdrawal and neuronal activity of lateral paragigantocellularis nucleus. *Behav Brain Res* 2021; **414**: 113450.

82 Severino AL, Mittal N, Hakimian JK, Velarde N, Minasyan A, Albert R *et al.* μ-Opioid Receptors on Distinct Neuronal Populations Mediate Different Aspects of Opioid Reward-Related Behaviors. *eNeuro* 2020; **7**: ENEURO.0146-20.2020.